



CHORUS

This is the accepted manuscript made available via CHORUS. The article has been published as:

Reduced Transport of Swimming Particles in Chaotic Flow due to Hydrodynamic Trapping

Nidhi Khurana, Jerzy Blawdziewicz, and Nicholas T. Ouellette

Phys. Rev. Lett. **106**, 198104 — Published 13 May 2011

DOI: [10.1103/PhysRevLett.106.198104](https://doi.org/10.1103/PhysRevLett.106.198104)

Reduced Transport of Swimming Particles in Chaotic Flow Due to Hydrodynamic Trapping

Nidhi Khurana,¹ Jerzy Blawdziewicz,² and Nicholas T. Ouellette^{1,*}

¹*Department of Mechanical Engineering & Materials Science,
Yale University, New Haven, Connecticut 06520, USA*

²*Department of Mechanical Engineering, Texas Tech University, Lubbock, Texas 79409, USA*

We computationally study the transport of active, self-propelled particles suspended in a two-dimensional chaotic flow. The point-like, spherical particles have their own intrinsic swimming velocity, which modifies the dynamical system so that the particles can break the transport barriers present in the carrier flow. Surprisingly, we find that swimming does not necessarily lead to enhanced particle transport. Small but finite swimming speed can result in reduced transport, as swimmers get stuck for long times in traps that form near elliptic islands in the background flow. Our results have implications for models of transport and encounter rates for small marine organisms.

PACS numbers: 47.52.+j, 05.45.-a, 47.63.Gd

In a wide range of natural and industrial situations, fluid flows transport particulate matter. In many cases, the particles are passive: they have no internal dynamics, and though they may not behave as true fluid elements due to inertial effects [1], their motion is completely prescribed by the fluid flow. But not all particles are passively advected; rather, they can be “active,” obeying equations of motion that include more than just fluid advection [2]. Particle activity can be biological [3], chemical [4], or mechanical [5]. In all of these cases, the dynamics of the particles are very different from their fluid-element counterparts, and the interaction of the active particles and the fluid flow can produce dramatically complex behavior.

Swimming organisms are one common example of an active particle. They are ubiquitous in natural flows, and range from self-motile microorganisms to macroscopic animals such as fish. For small organisms, a significant body of research has focused on the detailed propulsion mechanisms used by the swimmers in their low-Reynolds-number environment [3, 6, 7] and on the hydrodynamic interactions that couple different organisms and lead to pattern formation and macroscopic fluctuations of the fluid velocity [8–10]. Experiments have confirmed these effects, and can now describe the flows produced by microorganisms in detail [11–13]. Larger organisms (such as krill) may have a significant effect on the flow at high Reynolds numbers, and it has been suggested that their activity may produce a non-negligible contribution to the ocean kinetic energy budget [14–16]. Comparatively little work, however, has been done to understand the effects of nontrivial flow fields on swimming particles, even though the coupling between the fluid flow and the particle dynamics may lead to qualitatively new behavior. Examples of such effects include the concentration of swimming particles in the chaotic regions of an underlying flow [17] and the spontaneous formation of phytoplankton layers due to cell tumbling in stratified shear flow [18].

In this Letter, we use a simple numerical model to

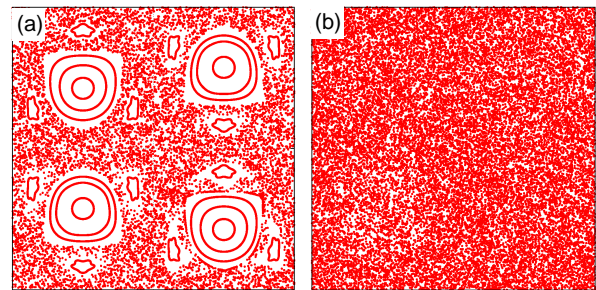


FIG. 1. (color online). Poincaré section for (a) fluid particles and (b) swimmers with an intrinsic speed of $v_s = 0.05$ in time-dependent flow ($B = 0.12$, $\Omega = 6.28$). High swimming velocity allows the swimmers to cross transport barriers that fluid elements cannot, and thus to explore the entire domain.

study the dynamics of swimming particles in a spatially nontrivial fluid flow that exhibits Lagrangian chaos. The particles are advected and rotated by the flow, and, in addition, they move with an intrinsic swimming velocity in a direction that depends on the instantaneous particle orientation. Despite the simplicity of this model (with only one-way coupling between the particle motion and the background flow) [17], we observe striking changes to the particle dynamics when they are self-motile.

Our two-dimensional background fluid flow is composed of a chaotic sea punctuated by elliptic islands; these islands are bounded by Kolmogorov-Arnold-Moser (KAM) tori that are impenetrable transport barriers for fluid elements. As expected, we find that even a small amount of motility allows the swimmers to cross these boundaries. Surprisingly, however, we find that swimming does not necessarily lead to uniformly enhanced transport. Rather, for a range of small but finite swimming speeds, the rate of particle transport can actually *decrease*. We connect this reduction of large-scale transport to the formation of “traps” that can hold the swimmers for very long times. These traps appear just inside

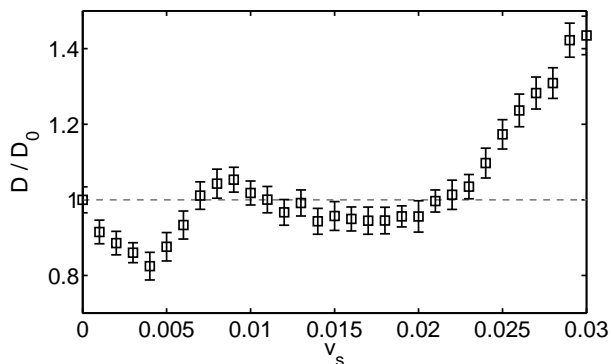


FIG. 2. Diffusion coefficient D scaled by D_0 , the diffusion coefficient for fluid elements, as a function of swimming speed v_s . Even though the swimmers tend to move faster than fluid elements, their long-time transport may be slower.

the boundaries of the elliptic islands of the underlying flow field, and each island has a distinct signature in the transport statistics. To show that these traps do indeed control the transport we computed conditional statistics, recovering the expected result of enhanced transport for swimmers that are outside of the traps. Our results have implications for models of encounter rates for small swimming organisms [19].

We advect our swimmers in a two-dimensional oscillating cellular flow given by the streamfunction

$$\psi(x, y, t) = \frac{U}{k} \sin[k(x + B \sin \Omega t)] \sin ky, \quad (1)$$

where U is the overall velocity scale, and k is the spatial wavenumber of the flow; B gives the amplitude of the lateral oscillation and Ω controls the time scale on which the flow field changes. This model flow is frequently used in studies of chaotic mixing [17, 20–23], and can also be approximated in the laboratory [24, 25]. For fluid elements, ψ plays the role of a Hamiltonian, with x and y as a conjugate position-momentum pair. When the flow is constant in time ($B = 0$), the dynamical system is integrable and fluid elements move on closed orbits within cells. Time dependence ($B \neq 0$), however, introduces the possibility of chaotic advection [26], as shown in Fig. 1(a) for $B = 0.12$ and $\Omega = 6.28$. This parameter choice leads to large period-1 elliptic islands enclosing the elliptic points of the flow and smaller period-3 islands surrounding them.

The swimmers themselves are modeled as non-interacting, pointlike, spherical particles with an intrinsic velocity vector \mathbf{u}_s . We assume that the magnitude of \mathbf{u}_s is fixed, though its direction may change. When flow is imposed, the velocity \mathbf{v} of the particle is the vector sum of the local fluid velocity \mathbf{u} and the swimmer’s intrinsic velocity, so that $\mathbf{v} = \mathbf{u} + \mathbf{u}_s$. Since the particles are spherical, they do not couple to the flow strain rate. They may, however, rotate with the flow vorticity, which

allows for reorientation of the intrinsic swimming velocity vector \mathbf{u}_s . The full equations of motion for the swimmers are thus [17]

$$\begin{aligned} \frac{dx}{dt} &= \frac{\partial \psi}{\partial y} + v_s \cos \theta, & \frac{dy}{dt} &= -\frac{\partial \psi}{\partial x} + v_s \sin \theta, \\ \frac{d\theta}{dt} &= -\frac{1}{2} \left(\frac{\partial^2 \psi}{\partial x^2} + \frac{\partial^2 \psi}{\partial y^2} \right), \end{aligned} \quad (2)$$

where we have nondimensionalized the equations with the characteristic length and velocity scales $1/k$ and U , respectively. We define a nondimensional swimming parameter as $v_s = u_s/U$; θ is the inclination of the swimmer velocity with respect to a fixed axis. We note that are our swimmers are qualitatively different from inertial particles [1].

Since the swimmer dynamics are no longer Hamiltonian, the particles may cross the KAM tori of the underlying fluid flow [17], exploring more of the flow domain than a fluid element can. To illustrate this enhanced mobility, we show in Fig. 1(b) the trajectory of a single swimmer with $v_s = 0.05$, stroboscopically sampled at the frequency of the flow (a Poincaré section). The swimmer is fast enough in this case to be able to explore the whole space; we find that for $v_s > 0.065$, a swimmer can be found anywhere with equal probability.

Even though swimming allows a particle to explore more of the domain, we find that their long-time transport is surprisingly not uniformly enhanced when compared with fluid elements. To illustrate this behavior, we measured the mean-square displacement as a function of time for fluid elements and swimmers initially in the chaotic sea. As expected, this mean-squared displacement scales diffusively [20]; that is, $\langle r^2 \rangle = 4Dt$, where r is the displacement of a particle from its initial position, D is a diffusion coefficient, and $\langle \cdot \rangle$ denotes an average over θ and initial positions in the chaotic sea. In Fig. 2, we plot the measured diffusion coefficients as a function of the swimming speed v_s . For $v_s < 0.025$, the long-time transport of the swimmers is not significantly faster than for fluid elements, and may actually be *slower*.

To understand this behavior, we studied the spatial dynamics of the swimmers. As noted above, fluid elements cannot cross the KAM tori in the underlying flow, and large regions of the phase space are therefore inaccessible to those moving in the chaotic sea. Very fast swimmers, in contrast, can uniformly explore the whole domain. Between these limits, however, the particle dynamics are markedly different. For $v_s \lesssim 0.03$, we find that the cores of the elliptic islands of the underlying flow remain inaccessible for particles that were initially in the chaotic sea, but that the swimmers *can* cross the KAM tori on their periphery. In the newly accessible regions just inside the elliptic islands, we observe a surprising phenomenon: the swimmers can become stuck for long times—sometimes thousands of flow cycles. During

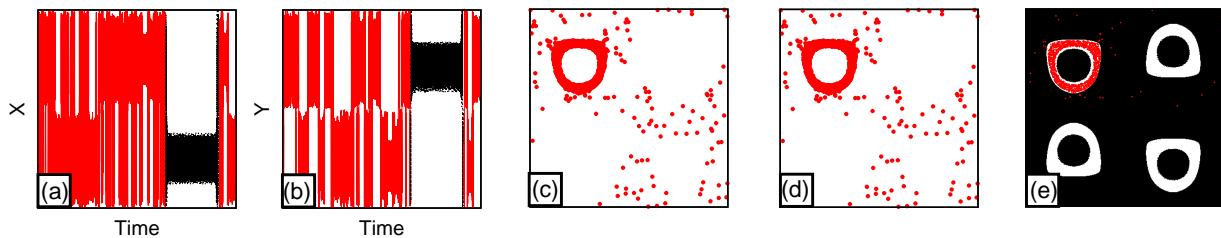


FIG. 3. (color online). Swimmer dynamics inside the traps, for $v_s = 0.01$. (a,b) x and y positions of a single swimmer as a function of time (measured in flow cycles), assuming periodic boundary conditions. In the black portion of the trace, the swimmer is stuck in a trap. (c) Poincare section of the swimmer in the black segment of the time trace. (d) Poincare section of the swimmer for the gray (red online) segment of the trace. (e) Locations of the traps (in white), for $v_s = 0.01$. The white regions are computed as the difference between the domain accessible to swimmers and that accessible to fluid elements. The dots show the same data as in panel (c).

these “trapping” events, the swimmer is constrained to remain inside the elliptic island and moves on an orbit that may remain bounded for a long time.

To illustrate this phenomenon, we show in Fig. 3 the time trace of the horizontal and vertical coordinates (assuming periodic boundary conditions) of a single swimmer with $v_s = 0.01$. These coordinates typically fluctuate rapidly as the swimmer moves chaotically, jumping between periodic cells of the underlying flow. Sometimes, however, the fluctuations decrease markedly, and the swimmer remains for a long time in a trap.

The existence of “sticky” regions that resemble the trapping regions observed in our simulations has been seen before in studies of Hamiltonian chaos, where the stickiness is associated with phase-space domains that are dense in elliptic-island chains [27]. Although we do observe some weak sticking for fluid elements very close to the elliptic islands, the interpretation of our observations for swimmers is different. Once swimming is introduced, the system is no longer Hamiltonian, and the trapping regions we observe are much larger than the regions that are sticky for fluid elements. The traps that form in our system are purely due to the interaction of the intrinsic swimmer dynamics with the underlying flow field.

Comparing Fig. 3(c) with Fig. 1(a), we see that the traps indeed form just inside the elliptic islands of the background flow. To identify the trapping regions in an automated way (so that we can make statistical measurements), we measured both the set Ω_f accessible to fluid elements and the set Ω_s accessible to swimmers for a given v_s . The set $\Omega_t \equiv \Omega_s - \Omega_f$ is then the region newly accessible for the swimmers. An example of Ω_t is shown in Fig. 3(e). We have also included the data shown in Fig. 3(c) on this plot; it is clear that the trapped particle remains in the region Ω_t .

To test the hypothesis that it is these traps that lead to the reduced transport, we measured the diffusion coefficients for swimmers while they were outside the traps, as shown in Fig. 4. To clarify the dynamics further, we separated Ω_t into the traps that form in the large period-

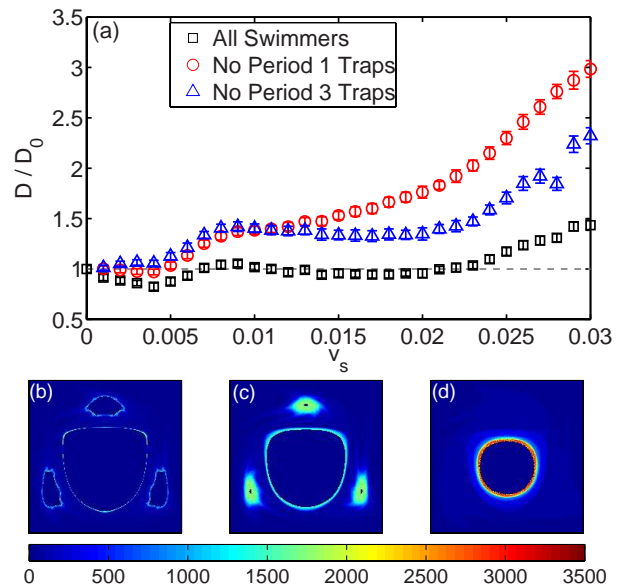


FIG. 4. (color online) (a) Diffusion coefficient for swimmers when they are outside of the traps. Data is shown separately for swimmers that are not in the large period-1 traps and the smaller period-3 traps. For comparison, the data from Fig. 2 for all the swimmers are also shown. (b-d) Spatially resolved maps of the mean time for a particle to cross a cell boundary, for (b) $v_s = 0$ (i.e., fluid elements), (c) 0.002, and (d) 0.01. Only one quarter of the unit cell of the flow is shown; the rest are related by symmetry. The color bar shows the time in flow cycles.

1 islands and those in the smaller period-3 islands. As is evident from Fig. 4, the addition of intrinsic swimming *does* enhance the transport, as long as the swimmers are outside the traps. The reduced transport we saw in Fig. 2 is due solely to the formation of traps, which, for small v_s , overwhelms the enhancement due to swimming.

Figure 4 also shows that the effect of the two different types of traps (the period-1 and period-3 islands) is not the same: slower swimmers are more affected by the period-3 traps, while faster swimmers feel the period-1

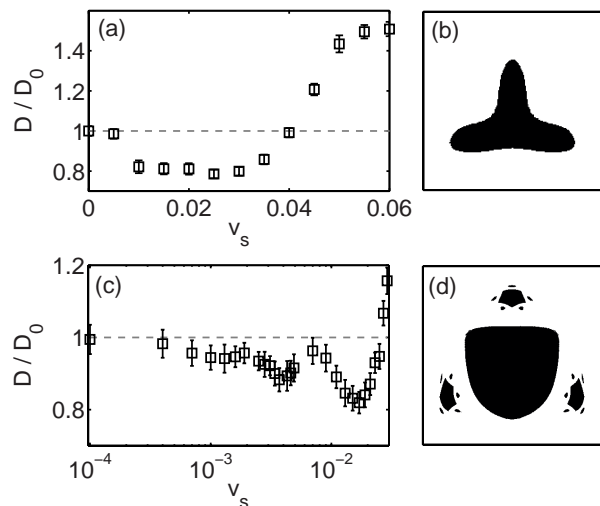


FIG. 5. Diffusion coefficients and elliptic islands for other sets of parameters. (a,b) For $B = 0.3$, we observe one dip in the diffusion coefficient as a function of v_s , corresponding to the single, period-1 elliptic island. (c,d) For $B = 0.14$, we observe three dips, one for each of the period-1, period-3, and period-5 islands.

islands more. This behavior is simple to explain. The transport boundaries surrounding the higher-period islands are weaker, and so the swimmers can enter them for smaller values of v_s . Therefore, even though the period-1 traps are stronger, the period-3 traps are *larger* for slow swimmers. For larger v_s , however, the period-3 traps are too weak to constrain the swimmers strongly, but the swimmers are fast enough to penetrate deeper into the period-1 traps. We demonstrate this effect in Fig. 4(b-d) by displaying spatial maps of the mean time a particle with a given initial position takes to cross a cell boundary. The results show that particles with small swimming velocity v_s are strongly affected by the period-3 islands, while those with larger v_s are only influenced by the period-1 islands, explaining the non-monotonic behavior seen in Fig. 2. As further confirmation, in Fig. 5, we show results for other flow parameters: $B = 0.3$, which gives only period-1 islands, and $B = 0.14$, which gives period-1, 3, and 5 islands. As expected, we find one minimum of D as a function of v_s for each type of island. These results suggest that the effects we see are quite general and will also be present in more complex flows, which may have elliptic islands of many different strengths and sizes and swimmers with many different swimming speeds: each elliptic island will act as a strong trap for *some* swimmers.

In summary, we have studied the interplay of motility and flow for self-propelled spherical particles advected by a chaotic flow. As expected, adding swimming enhances the overall mixing, in that the swimmers can explore more of the flow domain than a fluid element can. We found, however, that adding motility *does not* uni-

formly enhance particle transport; rather, for small but finite values of the swimming speed, motile particles can become stuck on nearly bounded orbits for long times. These traps form just inside the elliptic islands in the flow, and lead to weaker chaotic diffusion. In addition to this reduced transport, our results have implications for the estimation of encounter rates for swimming organisms, since swimmers may be more likely to find each other when they are constrained in a small region for long times. Finally, our results also show that some characteristic features of Hamiltonian chaos (such as the existence of elliptic islands and sticky regions) are approximately retained even under non-Hamiltonian perturbations.

We thank U. Feudel, E. Hernandez-Garcia, K. Mitchell, and T. Solomon for helpful discussions. J.B. acknowledges support from NSF grant CBET-1059745.

* nicholas.ouellette@yale.edu

- [1] M. R. Maxey and J. J. Riley, *Phys. Fluids*, **26**, 883 (1983).
- [2] Z. Toroczkai and T. Tél, *Chaos*, **12**, 372 (2002).
- [3] T. J. Pedley and J. O. Kessler, *Annu. Rev. Fluid Mech.*, **24** (1992).
- [4] J. R. Howse *et al.*, *Phys. Rev. Lett.*, **99**, 048102 (2007).
- [5] R. Dreyfus *et al.*, *Nature*, **437** (2005).
- [6] M. J. Lighthill, *Comm. Pure Appl. Math.*, **5** (1952).
- [7] E. Lauga and T. R. Powers, *Rep. Prog. Phys.*, **72**, 096601 (2009).
- [8] P. T. Underhill, J. P. Hernandez-Ortiz, and M. D. Graham, *Phys. Rev. Lett.*, **100**, 248101 (2008).
- [9] D. Saintillan and M. Shelley, *Phys. Fluids*, **20** (2008).
- [10] T. Ishikawa and T. J. Pedley, *Phys. Rev. Lett.*, **100**, 088103 (2008).
- [11] X.-L. Wu and A. Libchaber, *Phys. Rev. Lett.*, **84**, 3017 (2000).
- [12] K. Drescher *et al.*, *Phys. Rev. Lett.*, **102**, 168101 (2009).
- [13] K. C. Leptos *et al.*, *Phys. Rev. Lett.*, **103**, 198103 (2009).
- [14] W. K. Dewar *et al.*, *J. Mar. Res.*, **64**, 541 (2006).
- [15] J. O. Dabiri, *Geophys. Res. Lett.*, **37**, L11602 (2010).
- [16] J.-L. Thiffeault and S. Childress, *Phys. Lett. A*, **374**, 2487 (2010).
- [17] C. Torney and Z. Neufeld, *Phys. Rev. Lett.*, **99**, 078101 (2007).
- [18] W. M. Durham, J. O. Kessler, and R. Stocker, *Science*, **323**, 1067 (2009).
- [19] F. G. Schmitt and L. Seuront, *J. Mar. Sys.*, **70**, 263 (2008).
- [20] T. H. Solomon and J. P. Gollub, *Phys. Rev. A*, **38**, 6280 (1988).
- [21] A. Babiano *et al.*, *Phys. Rev. Lett.*, **84**, 5764 (2000).
- [22] T. Nishikawa, Z. Toroczkai, and C. Grebogi, *Phys. Rev. Lett.*, **87**, 038301 (2001).
- [23] R. Festa, A. Mazzino, and M. Todini, *Phys. Rev. E*, **80**, 035301 (2009).
- [24] D. Rothstein, E. Henry, and J. P. Gollub, *Nature*, **401** (1999).
- [25] N. T. Ouellette and J. P. Gollub, *Phys. Rev. Lett.*, **99**, 194502 (2007).

[26] H. Aref, *J. Fluid Mech.*, **143**, 1 (1984).

[27] M. Harle and U. Feudel, *Chaos Soliton Fract.*, **31**, 130 (2007).